RESEARCH ARTICLE

Bio-inspired synthesis of nanocrystalline calcite demonstrating significant improvement in mechanical properties of concrete: a construction-nanobiotechnology approach

Ankita Debnath[1] · Ritik Jeengar[2] · Damodar Maity[2] · Ramkrishna Sen[1]

Abstract

The bioinspired synthesis of construction material, known as biocement, represents a significant advancement in addressing the environmental sustainability issues associated with traditional cement use in the built environment. Biocement is produced through the process of microbially induced bio-mineralization (MIBM), which offers a promising alternative or supplement to conventional cement, potentially reducing its consumption. Despite extensive literature on the application of biocement in construction biotechnology, the fundamental mechanisms underlying its ability to enhance concrete quality remain poorly understood. This study focuses on the kinetics of biomineral synthesis by two *Bacillus* species; *Bacillus megaterium* RB05 and *Bacillus foraminis* DRG5, to identify the most effective strain for biomineralization. Bioconcrete specimens were created by adding inoculum containing *Bacillus megaterium* RB05 cells with a nutrient solution to the concrete mixture in a layer-by-layer approach. After 28 days of water curing, nanoparticles of $CaCO_3$, ranging in size from 27 to 82 nm, were produced in the bioconcrete specimens. The resulting concrete, containing nanocrystalline biogenic calcite, demonstrated significant improvements in mechanical properties. Specifically, compressive and tensile strengths of the bioconcrete, tested using a universal testing machine (UTM), increased by $7.69 \pm 0.08\%$ and $22 \pm 0.1\%$, respectively, after 72 h of curing. Additionally, the biocement was found to exhibit an organic–inorganic hybrid nature, as identified by TEM, EDAX, FESEM, FTIR, and XRD analyses. The enhanced mechanical properties were attributed to the high surface-to-volume ratio and hybrid nature of the calcite nanoparticles. The findings of this investigation are encouraging, suggesting the potential development of future green and self-sustainable construction materials or bioconcrete.

Keywords Bioinspired synthesis · Calcite nanoparticles · Green construction material · Kinetics · Improved mechanical properties · Built environment

Introduction

With the ever-increasing world population, demand for concrete production is also rising exponentially. The resulting increase in consumption of cement is responsible for the vast amount of carbon emission by the construction sector. Enormous carbon emission in the environment has taken a toll on the global climate, prompting the scientific community to indulge in research leading to a smaller carbon footprint. Among the global CO_2 emission sectors, construction and building materials contributes to almost 11%, which mostly occurs during production of construction material, cement (IEA 2017). This is because during the making of ordinary portland cement, vast amount of CO_2 gets liberated into the atmosphere contributing to greenhouse gas emission (IEA 2017; Labaran et al. 2022). Thus, bioconcrete has emerged as a modern urban solution for the construction industry to combat its alarming contribution in the global carbon footprint. Certain microorganisms by their extracellular mineral precipitation capability produces biominerals like calcium carbonate, that can be used for various purposes like repairing of

✉ Ramkrishna Sen
rksen@yahoo.com; rksen@bt.iitkgp.ac.in

1 Department of Bioscience and Biotechnology, Indian Institute of Technology Kharagpur, Kharagpur, West Bengal 721302, India

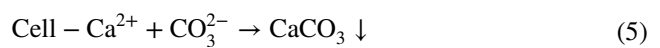2 Civil Engineering Department, Indian Institute of Technology Kharagpur, Kharagpur, West Bengal 721302, India
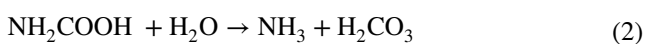
cracks in concrete (self-healing of cracks), CO_2 sequestration, soil improvement by strengthening and preventing erosion, bioremediation, and maintenance of heritage constructions (Zhu and Dittrich 2016; Mortazavi Bak et al. 2021; Dubey et al. 2023).

The process of making self-healing bio-minerals by microorganisms takes place by a phenomenon called microbial-induced bio-mineralization (MIBM), which involves a chain of metabolic reactions that leads to enzymatic degradation of urea to produce calcite or its different polymorphs. Bacterial extracellular polymeric substance (EPS), which is natural biopolymer, acts as the nucleation site for the crystallization to occur (Debnath et al. 2023; Tourney and Ngwenya 2009). EPS consists of certain biomolecules that chelates Ca^{2+} ions, thereby forming sites for crystal growth. Calcium carbonate precipitation takes place at the cell surface by successive stratification, alongside bacterial growth within the crystals (Debnath et al. 2023).

$CaCO_3$ biominerals are utilized mostly for the remediation of soil, concrete cracks, consolidation of heritage buildings, and monuments (Ortega-Villamagua et al. 2020). Bacteria produce these biomineral calcium carbonate by a number of biochemical pathways like photosynthesis, denitrification, sulfate reduction, methane oxidation, ammonification and ureolysis. Among which, ureolysis, is the most extensively studied process of MIBM due to its robustness and shorter reaction time (Harnpicharnchai et al. 2022; Debnath et al. 2023).

Following ureolysis, several microorganisms, mostly habiting in alkaline environments or in soil, has been found to have the potential to produce calcium carbonate minerals, extracellularly through a series of biochemical reactions. Thus, there is a drive to identify and utilize potent microorganisms amongst them, having efficient biomineralization ability. Literature mostly deals with *Bacillus sphaericus*, which has proven to be a good candidate for biomineralization, whereas the use of other bacterium for bioconcrete development seems less explored.

The entire process of ureolysis is carried out by urease, an enzyme produced by ureolytic bacteria. Following are the metabolic reactions that takes place during MIBM (Dhami et al. 2014; Anbu et al. 2016).

$$CO(NH_2)_2 + H_2O \xrightarrow{Urease} NH_2COOH + NH_3 \qquad (1)$$

$$NH_2COOH + H_2O \rightarrow NH_3 + H_2CO_3 \qquad (2)$$

$$H_2CO_3 \rightarrow CO_3^{2-} + 2H^+ \qquad (3)$$

$$2NH_3 + 2H_2O \rightarrow 2NH_4^+ + 2OH^- \qquad (4)$$

$$Cell - Ca^{2+} + CO_3^{2-} \rightarrow CaCO_3 \downarrow \qquad (5)$$

Calcium carbonate precipitation (CCP) in bacteria is also induced by few intracellular factors such as high pH, increasing amount of dissolved inorganic carbon (DIC), presence of divalent cations at the cell surface, and nucleation sites to chelate the divalent cations (Zhu and Dittrich 2016). It involves enzymatic decomposition of 1 mol of urea by bacterial cells to produce 1 mol of ammonia and 1 mol of carbamic acid. Subsequent hydrolysis of carbamic acid results in the formation of another 1 mol of ammonia and 1 mol of carbonic acid. These products then equilibrate in water to form 2 mols of ammonium ion, 1 mol of bicarbonate, and 2 mols of hydroxide ions, which increases the pH of the microenvironment. This alkaline pH shifts the bicarbonate equilibrium to form carbonate ions, which then combines with the calcium ions present at the surface of the bacterial cells to form calcium carbonate (Zhu and Dittrich 2016). Apart from urease, other enzymes like carbonic anhydrase, asparaginase (Li et al. 2015) also catalyzes the MIBM process, but so far urease has proved to be the most efficient for biomineralization.

Literature in the field of biocementation has mostly dealt with the application of few bacterial strains in bioconcrete development and further in self-healing of concrete, optimization of different parameters for efficient self-healing, thus mostly satisfying the environmental engineering application goals. However, from a biological point of view, the fundamental aspect of nature inspired biomineralization in bacterial cells has not yet been fully understood (Hoffmann et al. 2021; Carter et al. 2023). The current study aims to understand that whether the properties of bacterially produced biocement are inspired or derived from naturally occurring biominerals or not. Naturally occurring bio-minerals like seashells, rocks, etc. have much higher strength and durability than their inorganic counterparts like chalk although all of them are composed of $CaCO_3$ but the former ones have much higher strength due to the presence of biological moieties in them. These bio-minerals comprised of biological macromolecules such as proteins and other organic matters present in the crystalline matrix which converts the fragile calcium carbonate into hard and durable materials (Wegst et al. 2015). In case of microbial biomineralization, several studies have shown the presence of organic biomacromolecules associated with inorganic $CaCO_3$ (Enyedi et al. 2020; Khanjani et al. 2021; Debnath et al. 2023). It is essential to know whether the presence of these biogenic $CaCO_3$ when produced by the bacterial cells inside concrete enhances the compressive, tensile and flexural strength, by filling in the pores and voids present in concrete. Recent reports (Ahmed et al. 2021; Sarkar et al. 2023) have shown the improvement of bioconcrete mechanical properties over conventional concrete due to the precipitation of biogenic calcium carbonate by microbial cells. These studies report the filling of concrete microvoids by these

biomineral particles and reasoned that the increase of structural properties of bioconcrete is due to reduced water and chloride ion permeability through the biomineralized micropores. Many studies, in the last few years, have reported the optimization of microbial inoculum, nutrient concentration along with physical parameters like temperature, humidity to achieve higher yield of $CaCO_3$ thereby obtaining sustained strength of soil and concrete (Jiang et al. 2020; Alshalif et al. 2022; Dagliya et al. 2023; Benjamin et al. 2023; Onyelowe et al. 2024; Yu et al. 2022). While some studies have shown the effect of curing type such as water or air on the strength enhancement of bioconcrete, some has shown the effect of curing time on the same (Sumathi et al. 2020; Zheng et al. 2020). However, studies addressing the fundamental aspect of bioconcrete development are few, such as the role of microbial biomineral in enhancing the strength of bioconcrete has not been studied much. In addition, the contribution of organic moieties of biomineral towards the bioconcrete properties has not been considered so far. Thus, this study is an attempt to address the underlying chemistry of biocement properties in order to improvise the usability of this technique in construction industry. The core of this study lies in the identification of a better bacterial species for biocementation, and understanding its ability to improve the concrete quality through the formation of calcite nanoparticles.

Hence, the present study deals with the detailed process of microbially induced biomineralization (MIBM) in two indigenous alkaliphilic strains of *Bacilli* such as *Bacillus megaterium* RB05 and *Bacillus foraminis* DRG5. Selection of the potent MIBM bacterium was performed, along with characterization of the precipitated biomineral, through a number of analytical techniques. This study also includes the bioinspired development of concrete followed by its physico-mechanical and chemical characterization. The most interesting aspect of this study lies in the elucidation of the particle nature of the biomineral formed inside the bioconcrete. Investigation on the effect of the size of calcite particles, affecting the properties of concrete, has also been looked upon. In addition, the role of organic components associated with the $CaCO_3$ mineral in enhancing the strength of the bioconcrete has been discussed. Finally, an overview of comparative analysis of performance and cost between bioconcrete versus conventional concrete has also been performed in the end.

Material and methods

Biochemical parameters studied during MIBM

Bacterial inoculum and culture conditions

Bacillus megaterium RB05 and *Bacillus foraminis* DRG5 isolated from riverbank silt deposits from southern region of West Bengal, India, by Chowdhury et al. (2011) and Ghatak et al. (2013), were used in this study. The two strains were maintained on nutrient agar plates from which single colony was picked up and inoculated into 5 ml of nutrient broth (seed culture). These cultures were incubated at 30 °C in a rotary shaker at 150 rpm overnight. However, DRG5 did not show any growth so it was further incubated at 37 °C, 120 rpm overnight. Next day, the primary (seed) cultures were subcultured to make a secondary inoculum by inoculating 5% (v/v) overnight grown cultures were inoculated into 50 ml of nutrient broth media.

Selection of urease producing bacterial strain

Screening of the two bacterial strains for urease activity was done using Urea Agar Base (Christensen), Himedia. The media essentially comprises of nutrient agar supplemented with phenol red, as color indicator and is generally used to test bacterial cells for urease activity (Reeksting et al. 2020). The overnight grown cultures of BM RB05 and BF DRG5 were streaked onto urea agar base plates and incubated for 5 days without shaking condition at 30 °C and 37 °C respectively.

Two percent filter-sterilized urea was added to the agar medium after autoclaving, and *Escherichia coli* was used as the negative control. Color change indicated urease production which was observed every day throughout the incubation period for 5 days. A blank plate was incubated without any bacterial inoculation.

In-depth study of MIBM

To study the biochemical process of MIBM in an ureolytic bacterium *Bacillus megaterium* (BM) RB05, *Bacillus foraminis* (BF) DRG5 by growing cells in urea-$CaCl_2$ medium. BM RB05 cells maintained on nutrient agar plates were cultured on Nutrient broth Urea (NBU) medium. The media contained nutrient broth, 2% urea, 25 mM $CaCl_2$, and 5 μM $NiCl_2.6H_2O$ (Debnath et al. 2023). At first, a seed culture was prepared from which 10% (v/v) inoculum was added on to the production medium. The cultures were grown for 120 h and aliquots were withdrawn at every 24-h interval for analysis. Cultures were grown in triplicates. Control was prepared by growing BM RB05 cells in the presence of ammonium nitrate as nitrogen source to understand the role of urea in MIBM. Test samples were designated as RB05_Urea, DRG5_Urea, and control as RB05_Ammonium nitrate. All experiments were performed in three biological replicates ($n = 3$).

Time course profile of growth, pH, and enzyme activity

Since calcite precipitation occurs by increasing the pH of the microenvironment by generating hydroxide ions (Dhami et al. 2014), so it is important to study the pH change of the cellular microenvironment to mark the onset of the process. The pH of the medium was monitored at every interval of 24 h along with that the liberation of NH_4^+ ions by decomposition of urea was also monitored. The cell growth was monitored in terms of biomass concentration (g/L). The enzyme urease plays the pivotal role in this entire process by catalyzing the hydrolysis of urea thereby producing $CaCO_3$ by subsequent chain of reactions.

Electrical conductivity (mS/m) over time gives the rate of urea hydrolysis. The enzyme activity was calculated in terms of conductivity min^{-1}. Enzyme activity was calculated every 24-h interval till 120 h. Culture supernatants were added on to 1.1 M urea solution, change in electrical conductivity was calculated over a period of 5 min and then enzyme activity was calculated (Zoheir et al. 2013).

Biomineral production over time

Precipitation of biomineral $CaCO_3$ was studied at every 24-h interval till 24 h. Cultures of both BM RB05 and BF DRG5 were incubated for every 24-h interval and each set were taken out at regular interval and filtered through Whatman filter paper to collect the precipitate. The filtrates were extracted, dried by lyophilized, and weighed. Dry weights of precipitates were considered as the weight biomineral $CaCO_3$ (Harnpicharnchai et al. 2022).

Morphological characterization of cells during MIBM

Biomass samples were taken at every 24-h interval, lyophilized, and prepared for electron microscopy. Biomass samples were first centrifuged at 8000 rpm for 10 min; pellets were washed with 0.1 M phosphate buffer saline pH 7.4. This step was repeated twice, followed by fixation of biomass with 2.5% glutaraldehyde solution for at least 1 h in dark. Cells were again washed with PBS three times after which they were subjected to dehydration. The dehydration step was performed with an ethanol concentration gradient of 10–90% with 10% increment in each step. Cells were then incubated for 1 h in absolute ethanol (99.99%) followed by drop casting in 1 cm * 1 cm aluminium foil (Debnath et al. 2023). The foils with drop casted cells were kept under vacuum desiccation overnight; the next day, gold coating was performed before imaging. ZEISS EVO 60 scanning electron microscope with Oxford EDS detector with tungsten filament and maximum acceleration voltage of 30 kV was used.

X-ray diffraction for phase analysis

Since biomineral production was higher in case of BM RB05, the precipitates obtained from BM were characterized further. The culture broth of BM RB05 was filtered through a Whatman filter paper; insoluble precipitates of biomineral were collected in the filter paper. The precipitates were washed twice with distilled water at 8000 rpm for 15 min followed by freeze drying to obtain dried powders of the biomineral. Freeze-dried samples were analyzed for crystalline or amorphous nature of the biomineral as well as to identify phases of the biomineral. Powdered samples were mounted on stubs and subjected to high-resolution X ray diffraction in a Bruker AXS D2 PHASER with Cu Kα ($\lambda = 1.54$ Å) radiation source. 2θ was kept from 5 to 90 °C. Resulting X-ray diffractograms were analysed through Match! Software version 3.3 to identify the polymorphic phases. Crystallinity index was calculated using the following formula.

$$\text{Crystalinity index} = \frac{\text{Area of crystalline peaks}}{\text{Area of crystalline and amorphous peaks}} \tag{6}$$

Field emission scanning electron microscopy

Freeze-dried biomineral samples were diluted in absolute ethanol 1000 times to obtain a very dilute suspension was obtained. Diluted biomineral suspension in absolute ethanol was then drop casted in a 1 cm * 1 cm aluminium foil (Debnath et al. 2023). Samples were then stored under vacuum desiccation overnight followed by gold coating and imaging under MERLIN FESEM ZEISS equipped with GEMINI II column.

Development of bioconcrete

Concrete mortar specimens in the form of cylinders (of size 150 mm diameter and 300 mm long) and cubes (15 cm × 15 cm × 15 cm as per IS 10086–1982) were casted by adding OPC, fine aggregate, coarse aggregate having mix proportion of 1:1:2 with water cement ratio 0.40. Bacterial cells of *Bacillus megaterium* RB05 were inoculated in three layers during casting of the concrete mix, in specific molds of cubes and cylinders. Then, 2% (w/v) bacterial inoculum of the weight of the cement was added. BM RB05 cells were initially grown on nutrient broth containing 5 μM $NiCl_2.6H_2O$ to induce the urease activity in cells. Then, 24-h-old cultures having OD 1.5 were then subjected to concrete mixtures along with 2% urea and 25 mM $CaCl_2$. Specific concrete composition can be found in the following tables (Tables 1, 2, and 3).

Physico-mechanical properties of concrete

After 24 h, the specimens were demolded and subjected to water curing. Concrete mortar specimens of cylinders and cubes were given sufficient time for hardening were cured for 3, 7, 14, and 28 days. On each of these test days, cubes and cylinders were subjected to compressive and tensile strength measurement with the help of universal testing machine (UTM) tested for maximum load. The compressive strength was calculated using the following formula:

$$\text{Compressive Strength (N/mm}^2) = \frac{\text{Ultimate load}}{\text{Cross sectio area of specimen}} \tag{7}$$

For evaluating spilt tensile strength, cylinders were taken allowed to dry and tested in compression testing machine by placing the specimen horizontal. The ultimate load of the specimen falls horizontal. The ultimate load of the specimen is at which the cylinder failed. The following equation has been used for calculating tensile strength:

$$\textit{Tensile stress}(N/mm^2) = \frac{2P}{\pi DL} \tag{8}$$

Moreover, the stress value is obtained in N/mm². P is the ultimate load at which the cylinder fails. D and L are the diameter and length of the cylinder. Compressive strength calculated by dividing maximum load by the cross- sectional area.

Along with bioconcrete (concrete with bacterial inoculation), controls were made with conventional concrete without any bacterial inoculation, which were also tested for both compressive and tensile strength to have a comparative performance evaluation of bioconcrete.

Extraction and characterization of biomineral produced during MIBM in concrete

Biomineral produced by MIBM were subjected to material characterization by extracting samples after biomineralization in concrete. After strength analysis, precipitated samples were scraped out and subjected to further characterization.

Table 1 Conditions and specifications of concrete specimens

Indian standard method design stipulations	
Concrete grade	M25
Exposure	Mild
Quality control	Fair
Size of aggregate	20 mm
Cement used	OPC 53 grade cement
Sand grading zone	III

Table 2 Physical properties of concrete specimens

Material	Specific gravity	Bulk density (kg/m³)
Cement	3.14	1450
Fine aggregates	2.7	1650
Coarse aggregates	2.7	1575
Water		1000

Before analyzing, the biomineral samples were washed twice with distilled water to remove any interfering impurities.

X-ray diffraction analysis

After 28th day of curing and testing, the samples were scraped out from both bio concrete and normal concrete for chemical characterization. X-ray diffraction analysis was performed for both the samples to confirm the presence of calcium carbonate biomineral in bioconcrete. 2 θ was considered from 0 to 100 °C in HR-XRD, Bruker AXS D2 PHASER with Cu Kα ($\lambda = 1.54$ Å) radiation source. Results were analysed using Match! Version 3.3 and Origin Pro 8.5 software.

Energy-dispersive X-ray analysis

In order to identify the biomineral, it becomes inevitable to elucidate and identify the elements that it is made of. The insoluble precipitates of the biomineral were subjected to elemental composition analysis of through energy-dispersive X-ray analysis (EDAX) in EDAX Ametek connected to Zeiss MERLIN FESEM Gemini II.

Transmission electron microscopy

For TEM, biomineral samples were diluted 1000 times in isopropanol followed by sonication for 90 min. Samples were then drop casted in carbon coated Cu grids, vacuum desiccated and subjected to analysis in JEOL TEM.

Fourier transform infrared spectroscopy FTIR analysis was performed for the presence of organic groups in the precipitate by analyzing the functional groups present in

Table 3 Quantity of material per m³ of concrete

Material	Weight basis(kg)	Volume(m³)
Cement	425.73	0.294
Fine aggregates	539.54	0.327
Coarse aggregates	1231.77	0.782
Water	191.58	0.191

EPS components like polysaccharides, proteins, organic acids, etc. and to elucidate their role in the polymorph formation (Khanjani et al. 2021; Debnath et al. 2023). The freeze-dried samples were subjected to FTIR analysis after mixing with KBr pellets; the spectra were recorded from 400 to 4000 cm^{-1} in a Nicolet 670 Fourier transform infrared spectrometer.

Statistical analysis

All the experiments were performed in triplicate as mean $\pm$ standard deviation (S.D.) and were analysed through Origin Pro software version 8.5. The values of $p < 0.05$ were considered as statistically significant.

Results and discussion

Selection of urease producing bacterial strains

Urease being the crucial enzyme for when studying biomineralization through ureolytic pathway is an important parameter to investigate while delving into microbial biomineralization. The two strains *Bacillus megaterium* RB05 and *Bacillus foraminis* DRG5, in this study, were assayed for their ability to produce this enzyme, before proceeding into further experiments.

As observed from Fig. 1, both BF DRG5 and BM RB05 cells were found to produce urease enzyme as the color of the medium turned pink from orangish yellow. The colour of urea agar base medium turns pink due to the presence of phenol red that turns pink at an alkaline pH while retaining its original colour (orangish yellow) at neutral pH and turns yellow at acidic pH (Brink 2010). From Fig. 1, it was seen that BM RB05 and BF DRG5 produced urease consistently when incubated for 5 days. On the other hand, *E. coli* cells when incubated for 5 days turned the medium color yellow due to the production of organic acids during its growth, that turned the pH of the medium acidic. This also signifies that a non-ureolytic bacteria like *E. coli* turns the urea agar base acidic, while ureolytic ones like *Bacillus megaterium* RB05 and *Bacillus foraminis* DRG5 turns the medium basic due to the production of urease. The production of urease results in the hydrolysis of urea, producing ammonia and carbamic acid (Eq. 1). The ammonia produced gets protonated from water to produce ammonium ions, generating OH^{-} ions (Eq. 4) that increases the pH of the medium toward alkalinity, thereby turning the colour phenol red in the urea agar base medium into pink.
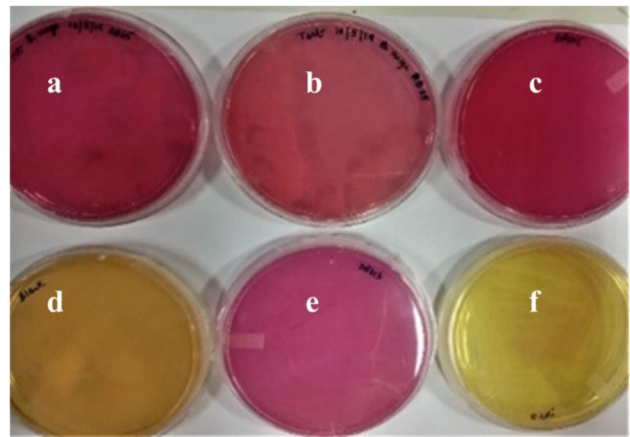

Fig. 1 Selection of urease producing cells on Urea agar base medium. **a** BM RB05 cells after 5 days. **b** BM RB05 cells after day 1. **c** DRG5 cells after 5 days. **d** Blank without bacterial inoculation. **e** DRG cells after day 2. **f** *E. coli* cells after 5 days

Biochemical parameters studied during MIBM

On confirming the ureolytic potential of both BM RB05 and BF DRG5, the biochemical parameters related to biomineralization were studied in detail. From the above figure (Fig. 1a–e), it can be suggested that with progress in cell growth, pH of the medium also rises, which indicates the ongoing process of microbially induced biomineralization. On studying the growth of both the bacterium during biomineralization, it was found that *Bacillus megaterium* RB05 and *Bacillus foraminis* DRG5 had similar cell growth pattern (Fig. 2a). Although biomass production was lesser in the case of BF DRG5 as compared to BM RB05, which can be due to better adaptability of BM RB05 in the biomineralization medium. Both the strains remained in logarithmic phase of growth till 24 h after which it remained in stationary phase till 120 h. As observed from Fig. 2b, the pH of the medium in case of both the bacterium increased steeply from 0 to 24 h; after 24 h, the pH of the biomineralization medium remained almost constant till 120 h. This is due to the active hydrolysis of urea during the log phase of growth, that results in the generation of hydroxyl ions, thereby raising the pH. During the stationary phase that from 24 to 120 h, the enzyme kinetics also reaches a saturation resulting in no further increase of pH. On the contrary, BM RB05 cells when grown in biomineralization medium with ammonium nitrate as the nitrogen source (without urea), no rise in pH was observed. It must to be noted that the starting pH in all three cases were same, 6 which increased to around 8.8 in case of BF DRG5 and 9.2 in case of BM RB05 but remained at 6.0 or slightly increased to 6.2 in ammonium nitrate containing biomineralization medium.

The main reason behind the differential pH profile during biomineralization under different nitrogen sources is that in
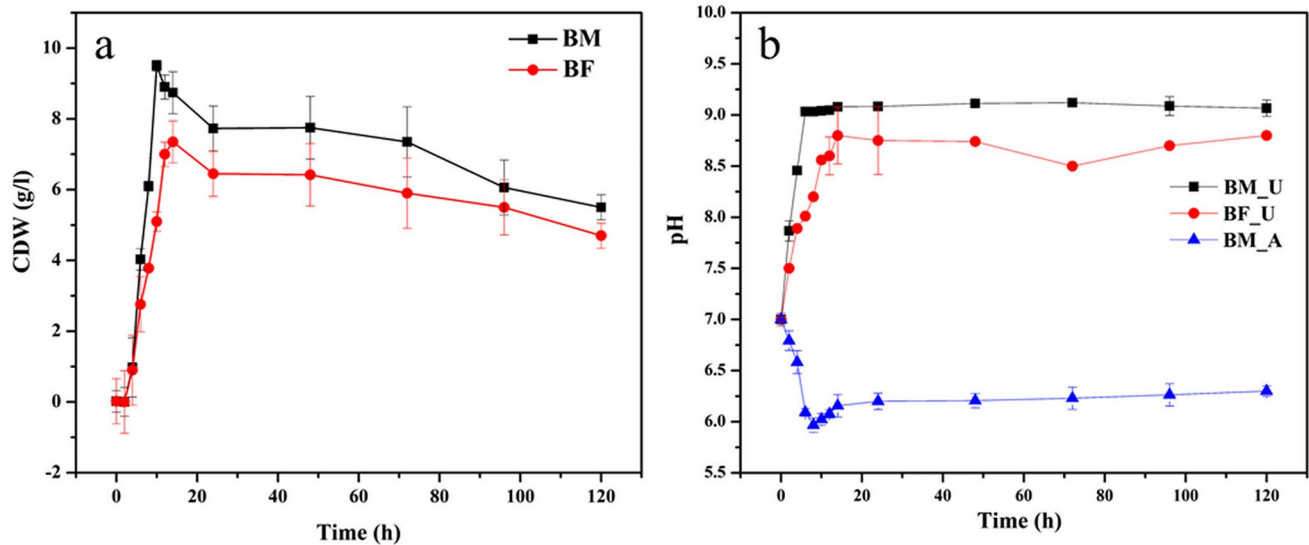
Fig. 2 a Time course growth profile of BM RB05 and BF DRG5 corresponding to *Bacillus megaterium* RB05 and *Bacillus foraminis* DRG5 respectively. **b** Time course pH profile of RB05_U, DRG5_U, and RB05_A corresponding to growth of RB05 and DRG5 cells un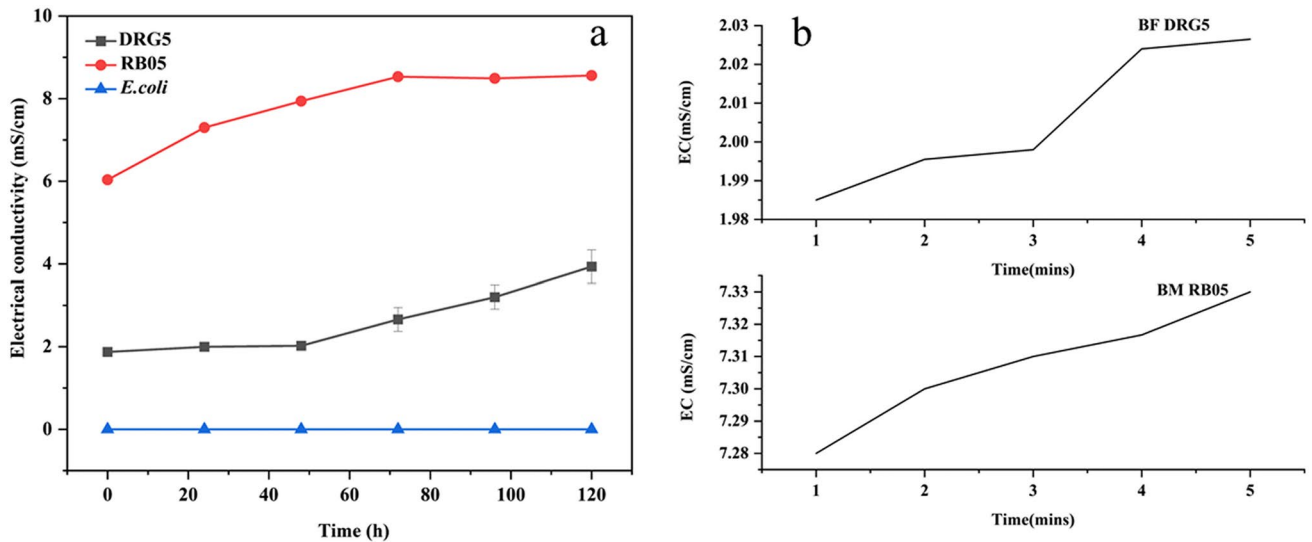der the presence of urea as biomineralization substrate and ammonium nitrate as the substrate respectively. All experiments were performed in biological replicates of three ($n = 3$)

the presence of urea, bacterial cells expresses an enzyme called urease that actively catalyze the hydrolysis of urea into ammonia andcarbamic acid (Dhami et al. 2014; Anbu et al. 2016; Mekonnen et al. 2021). The rise in pH is due to the generation of ammonium ions that shifts the bicarbonate into carbonate ions, this chain of metabolic reactions raises the pH to 9.5 as reported in case of widely studied MIBM strain *Sporosarcina pasturii* (Kim et al. 2018). In our case, it was observed that biomineralization in BF DRG5 cells increased the pH to 8.8 after which, it remained constant. This was a limitation of its biomineralization potential which we have later found in this study. BM RB05, on the other hand, has shown good biomineralization potential as the pH increased above 9. Further in this study, we could examine the biomineralization potential of these two bacteria.

Enzyme activity during MIBM

For analysis of urease activity, the electrical conductivity method was used (Mekonnen et al. 2021), where electrical conductivity (mS/m) over time gives the rate of urea hydrolysis. As seen, an increasing trend in urea hydrolysis correlates to higher urease activity. The enzyme activity was calculated in terms of conductivity min^{-1}. Electrical conductivity was calculated over a period of 5 min and then enzyme activity was calculated.

A distinct difference in the time course enzyme activity profiles of BM RB05 and BF DRG5 was seen (Fig. 3a). It was observed that BM RB05 had a much higher amount of enzyme right from 12 h of biomineralization, which was not observed in case of BF DRG5. Rather the increase in enzyme activity with time was found to be quite slow in BF DRG5 cells. For BM RB05 cells, the enzyme activity increased till 72 h after which it remained almost constant. However, for BF DRG5 cells the enzyme activity with time remained constant till 48 h and started to rise after that which kept on increasing till 120 h of biomineralization. On the other hand, no urease activity was seen in *E. coli* cells which also corroborated with the results obtained in urea agar base medium. From Fig. 3b, the enzyme activities of BM RB05 and BF DRG5 were found to be as 0.02 and 0.01 mS min^{-1}. As was observed form Fig. 3b, the electrical conductivity per min increased steeply in case of BM RB05 while, in case of BM DRG5 the electrical conductivity per min initially increased slowly followed by a stationary phase. The activity then increased sharply succeeded by a constant phase. The enzyme activity profiles can be well corroborated with the growth and pH profiles (Fig. 2a, b), in the logarithmic phase of cell growth, a rise in pH can be observed, likewise in similar pattern was observed for urease activity. Rise in urease activity from 0 to 24 h causes the pH rise in the same time frame, while during enzyme activity saturation the pH increase became stagnant. Thus, growth, urease activity and pH profile of both RB05 and DRG5 corroborated well with each other during the process of biomineralization.

Fig. 3 **a** Time course enzyme activity profiles of BM RB05, BF DRG5, and *E. coli* corresponding to growth of BM RB05 and BF DRG5 cells under the presence of urea as biomineralization substrate. **b** Enzyme activity calculated as electrical conductivity per min over a period of 5 min
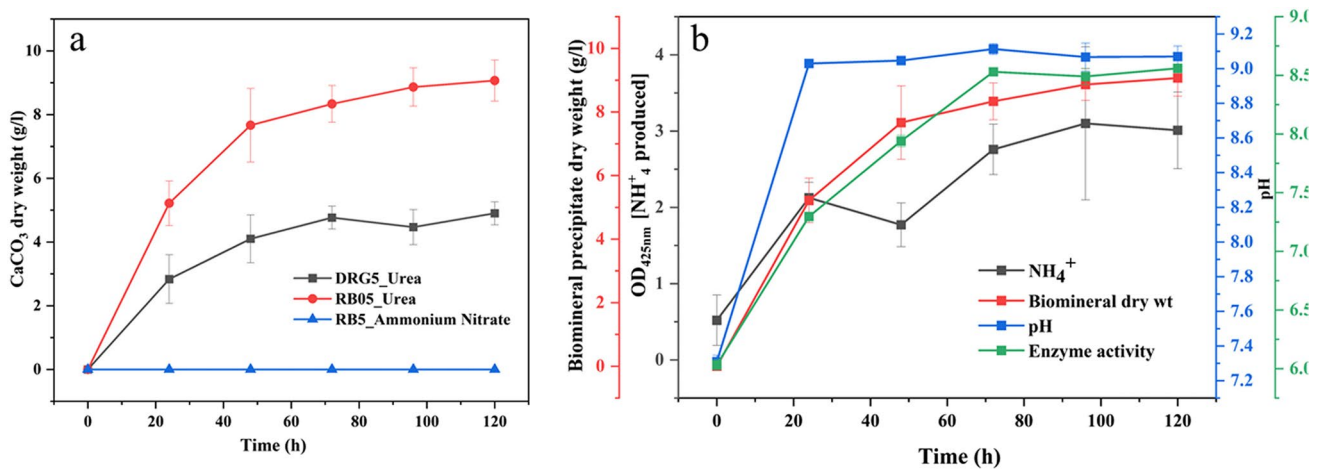
Fig. 4 **a** Time course biomineral production in RB05_Urea, DRG5_Urea, and RB05_Ammonium nitrate corresponding to growth of BM RB05 and BF DRG5 cells under the presence of urea and ammonium nitrate as the substrate of biomineralization respectively. **b** Representation of all the biochemical parameters studied in BM RB05 during biomineralization

Biomineral production over time

A production profile of biomineral with time, from 0th hour to the 120th hour was made, an increasing trend was observed in BM RB05, which is indicative of the fact that BM RB05 is a potent microorganism for biomineralization. A maximum yield of 9.06 g/L was observed after 120 h for RB05_U (Fig. 4a). BF DRG5 had a yield of fairly 4.9 g/L (Fig. 4a) and RB05_A, i.e., RB05 cells grown with ammonium nitrate as the nitrogen source, did not show any production of biomineral as no insoluble precipitate was found.

This is because, in the absence of urea, both ammonium and carbonate ions are not formed to produce calcium carbonate biomineral. This also signifies the importance of urea as a substrate for biomineralization. Performance of BM RB05 cells in biomineralization in comparison to BF DRG5 cells are better in terms of yield of the product. It suggests that since the bacterium has a higher enzyme activity and a fairly high yield of calcium carbonate, it seems a potent microorganism for applications like concrete and soil remediation. Figure 4b represents the profiling of all the biochemical parameters studied in BM RB05 during biomineralization. Additionally, it also shows the evolution

Table 4 Comparison of calcifying potential of different bacterial species with time

Microorganism	Calcifying potential	No. of days	Reference
Bacillus sp. *rMM9*	0.104 g L−1	21	Meier et al. (2017)
Agrococcus jejuensissMM 51	0.096 g L−1	21	Meier et al. (2017)
Bacillus muralis rLMd	0.064 g L−1	21	Meier et al. (2017)
Bacillus megaterium SS3	0.0187	21	Dhami et al. (2013)
Bacillus sp. CR2	2.32 mg/mg of cell dry weight	7	Achal and Pan (2014)
Bacillus cohnii	10.6% w/w of sand column	10	Liang et al. (2022)
Paenibacillus alkaliterreae	2.2 g L−1	7	Debnath et al. (2023)
Bacillus simplex BaSD-223 *Rhodococcus degradans* BaTD-248, *tenotrophomonas maltophilia* BaSD-214	10–20% per colony	182	Enyedi et al. (2020)
Bacillus subtilis	3.9 g L−1	7	Li et al. (2023)
Sporosarcina pasteurii	190 mg (approx.)	4	Gilmour et al. (2024)
Bacillus megaterium RB05	9.06 g L−1	5	This study
Bacillus foraminis DRG5	6.5 g L−1	5	This study

of ammonium ions with time, which corroborates with the pH profile and enzyme activity of the cells, as all of these biochemical parameters are directly related to each other. Table 4 shows the calcifying potential of different isolated bacterial strains with time. The calcifying potential of the two *Bacilli* strains from this study were also compared with literature (Table 4); from there, it can be observed that *Bacillus megaterium* RB05 and *Bacillus foraminis* DRG5 produced the maximum amount of calcite biomineral at the least amount of time, within 5 days. Hence, it was conferred from the results that these strains are quite potent to be used in bioconcrete structures for efficient production of the biomineral inside the concrete. Moreover, it can be said that, in only 120 h, the *B. megaterium* cells were able to produce 9.06 g/L of the biomineral, which is quite a high amount in a very short duration of time. Thus, this strain of *Bacillus* can yield impressive results in bioconcrete and other environmental engineering applications in future.

Morphological characterization of cells during MIBM

As observed from Fig. 5a–e, precipitation of biomineral was found around the BM RB05 cells from 0 to 72 h of biomineralization. At 0 h (Fig. 5a), no precipitation was seen around the cells, with progression of time from 12 h (Fig. 5b) production of biomineral could gradually be seen. This can be also be corroborated with biochemical results where cell was seen to actively express urease in the same time frame. Around 24 h (Fig. 5c), higher amount of biomineral accumulation was seen which was followed with copious biomineral deposition outside the cells within 72 h (Fig. 5d, e). This data was corroborated with Fig. 4a where the profile of time dependent production of biomineral showed that insoluble precipitates started to form after 12 h and with increasing time precipitation increased at a rapid rate.

However, in the case of *Bacillus foraminis* DRG5, the precipitation of biomineral was much slower when compared to BM RB05. Both time course biomineral precipitation (Fig. 4a) and SEM images (Fig. 6a, d) can correlate with the fact that biomineral production in BF DRG5 occurs at a much lesser rate in RB05. Also, distinct precipitates of biomineral cannot be found around the BF DRG5 cells from 0 to 72 h rather cells were seen clumped together in a matrix like structure. This matrix or mat-like structure encasing the cells was due to the presence of both bacterial extracellular polymeric substance (EPS) and biomineral. As reported by Khanjani et al. (2021) and Debnath et al. (2023) bacterial EPS plays a vital role in the biomineral precipitation process and that excessive production of these EPS molecules hinders the formation of biomineral resulting in lower precipitation rates. This might be the case for BFDRG5 as much lower quantity of biomineral precipitated in comparison to BM RB05 cells, where copious amount of precipitates was seen by the end of 72 h and kept on increasing till 120 h.

The precipitation of biominerals surrounding the cells with progression of growth was well observed for both the bacterium. Since biomineralization is essentially a crystallization process, the crystal nuclei form at the very beginning during the initial hours of growth (Debnath et al. 2023). Crystals continue to grow on the nucleus during the stationary phase after which it becomes constant. The growth of these crystals around the cells is dependent on the concentration of calcium and carbonate ions on the cell's exterior. The concentration of these building blocks of biomineral is dependent on the rate of urea hydrolysis by the cells as well as on the composition of the biomineralization medium. Thus, extracellular production of the biomineral is highly dependent on the growth of the cells and medium design.
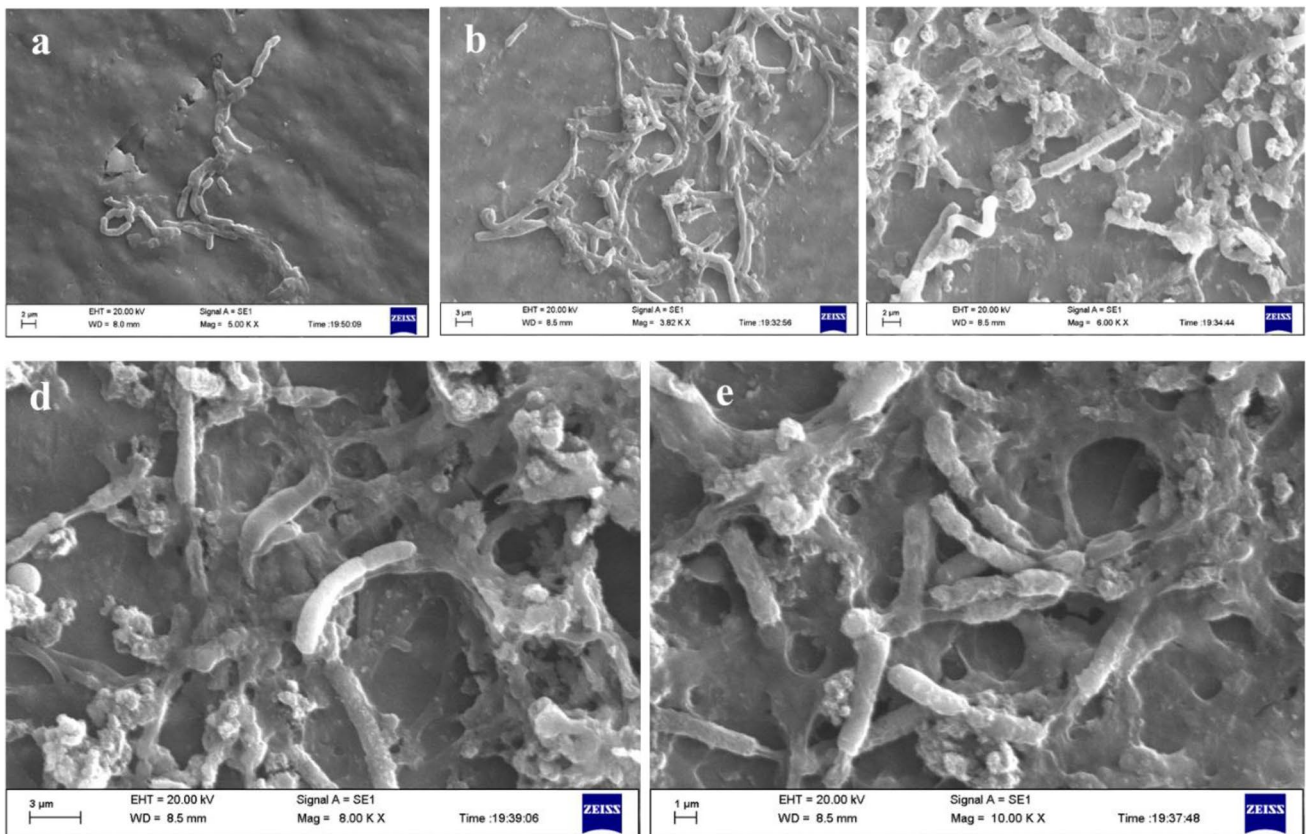
Fig. 5 SEM images of time dependent biomineralization in *Bacillus megaterium* RB05 cells at **a** 0 h, **b** 12 h, **c** 24 h, **d** 48 h, and **e** 72 h

## X-ray diffraction for phase determination of biomineral

X-ray diffraction reveals the phase of a material; it is done to analyze crystalline or amorphous nature as well as gives an understanding of the crystal lattice structure of a material. In this study, X-ray diffraction has been performed to analyze the phase of the biomineral precipitated by bacterial cells. The data was analyzed through Match! version 3.3 and Origin Pro version 8.5 software. As observed from Fig. 7, a sharp crystalline peak of calcite was observed at two theta 29.4 °C with the most stable plane of calcite (Rui and Qian 2022) at *hkl* value104 followed by several peaks of vaterite and calcite at other planes. The crystallinity index of the biomineral was found to be 81.28%. This suggests that the calcium carbonate biomineral is highly crystalline in nature with the major polymorphic phase as calcite. Although few planes of vaterite could also be observed, that might due to the presence of the vaterite, during phase transformation of the biomineral into calcite.

The presence of the most stable phase calcite as the predominant polymorph in the biomineral mixture was mostly due to the transition of the intermediate polymorphic phases to the thermodynamically stable form without any steric hindrance from the extracellular polysaccharides and proteins secreted outside the cells (Debnath et al. 2023). The extracellular polysaccharides and proteins mainly form the template for biomineral nuclei, initiating the process of crystallization. The crystallization further proceeds from amorphous calcium carbonate (ACC) to metastable vaterite to aragonite to calcite. During this transition often, excess bulky organic moieties of the bacterial extracellular surface causes steric hindrance preventing further crystallization of calcite, thereby arresting the vaterite phase (Khanjani et al. 2021; Debnath et al. 2023). In our previous study (Debnath et al. 2023), it was seen that due to lesser production of these bulky organic moieties in ureolytic pathway, the stable calcite polymorph of the biomineral stabilized, that can be corroborated with the results obtained in this study.

Field emission scanning electron microscopy

Insoluble precipitates obtained at the end of biomineralization were subjected to microscopic analysis to reveal the structural details of the mineral. Structural and morphological identification is necessary for identifying the nature of the biomineral. As observed from Fig. 8a, b, rhombohedral
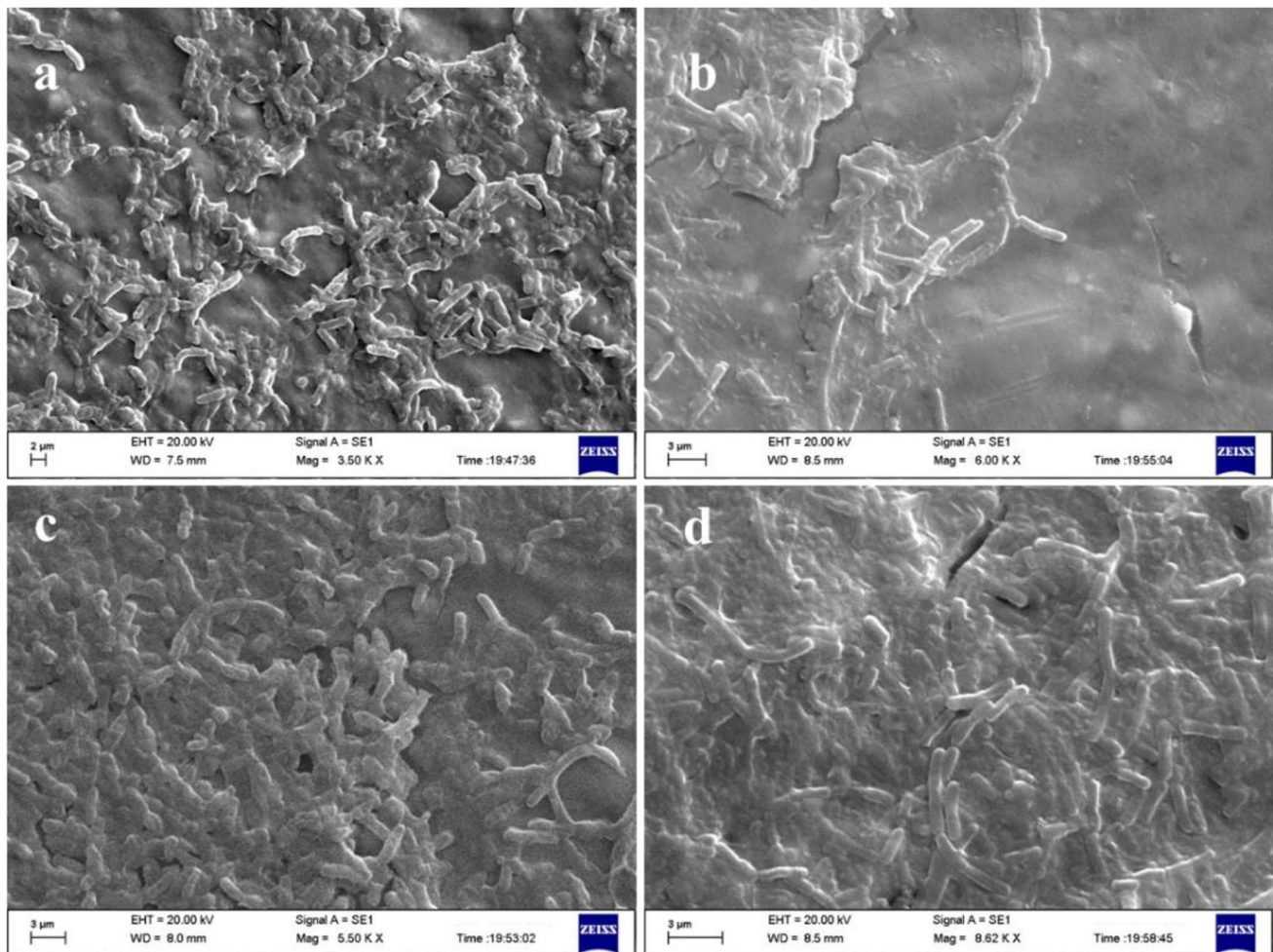
Fig. 6 SEM images of time dependent biomineralization in *Bacillus foraminis* DRG5 cells at **a** 0 h, **b** 24 h, **c** 48 h, and **d** 72 h
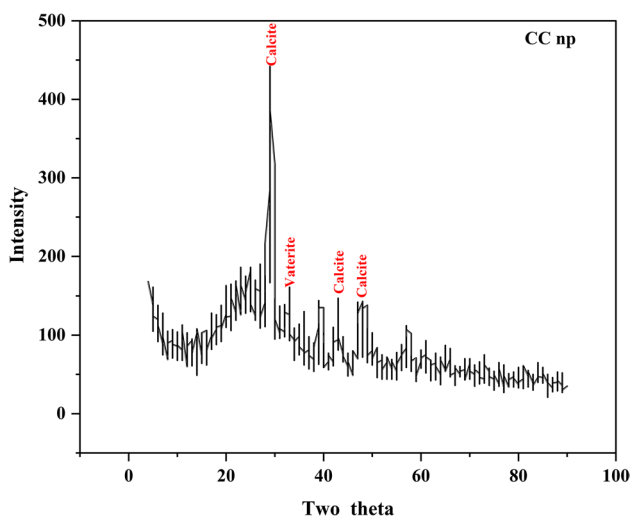
Fig. 7 X-ray diffractogram of calcium carbonate nanoparticles (CC np) produced extracellularly by bacterial cells

particles, which are typical characteristic morphological feature of calcite phase of calcium carbonate mineral, are observed. This entails the fact that the biomineral is produced as calcite, the most thermodynamically stable phase of calcite (Radha et al. 2010; Karthika et al. 2016). Formation of calcite phase of calcium carbonate mineral becomes essential for application in construction biotechnology as other phases of calcium carbonate like vaterite and aragonite are metastable phases having hydrophilic and porous nature that are suitable for applications in tissue engineering and regenerative medicine (Salomão et al. 2017).

Figure 8c shows a spherical structure of the biomineral, on further magnification in FESEM rhombohedral shaped outgrowths on surface of the sphere was seen. This might be due to the fact that formation of calcite is preceded by the formation of vaterite which mostly has a spherical structure (Andreassen 2005; Khanjani et al. 2021). With progression of time during biomineralization, these vaterite molecules get transformed into stable calcite. In the present study also, rhombohedrons like calcite structures were found to
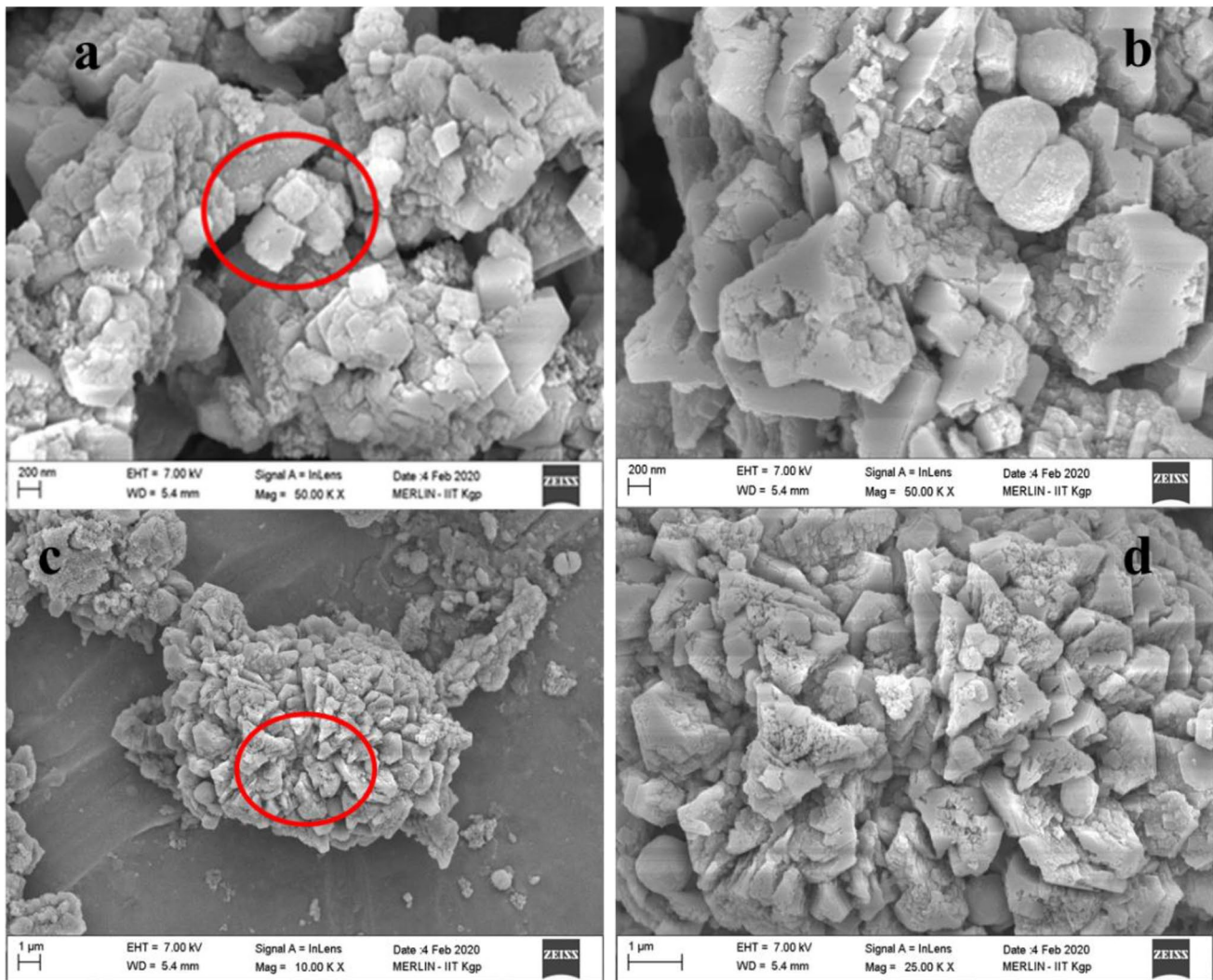
Fig. 8 a, **b** FESEM images of biomineral showing rhombohedral geometry of calcite. **c** Spherical shaped biomineral particle. **d** Magnified image of **c** showing calcite like outgrowth from spherical biomineral

be formed over the surface of spherical vaterite that suggests biomineralization proceeds with the formation of amorphous calcium carbonate to vaterite and finally to calcite.

Physico-mechanical properties of bioconcrete

The compressive and spilt tensile strength of bioconcrete was examined by casting bioconcrete in the form of cubes and cylinders respectively (Fig. 9a, b). The compression test is used to determine the hardness of cubical and cylindrical specimens of concrete. The strength of a concrete specimen depends upon cement, aggregate, bond, water-cement ratio, curing temperature, and age and size of specimen. Mix design is the major factor controlling the strength of concrete.

In the present study, it has been observed that right from the 3rd day of curing, the compressive strength of bioconcrete has increased (Fig. 10a) as compared to conventional concrete. The increment started from $7.69 \pm 0.08\%$ which ended up to $6.90 \pm 0.2\%$ at the end of 28 days. This signifies that the bacterial cells inside the concrete have undergone metabolic processes to produce $CaCO_3$ extracellularly, which has filled in the hydration pores present throughout the concrete structure and as a result, enhanced compressive strength was observed. On the other hand, the split tensile strength (Fig. 10b), which is indirect way of finding the tensile strength of concrete by subjecting the cylinder to a compressive force, also improved in case of bioconcrete.

This means that during the curing period, water ingression through concrete allowed the bacterial cells to grow and metabolize to produce the biomineral, thereby filling the micropores of concrete and increasing the strength of the structure. Sarkar et al. (2023) also observed similar results in

Fig. 9 Bioconcrete in the form of cubes and cylinders **a**, **b** after curing. **c** Bioconcrete subjected to load in UTM for evaluating compressive strength d. Bioconcrete interior structure after strength measurement in UTM
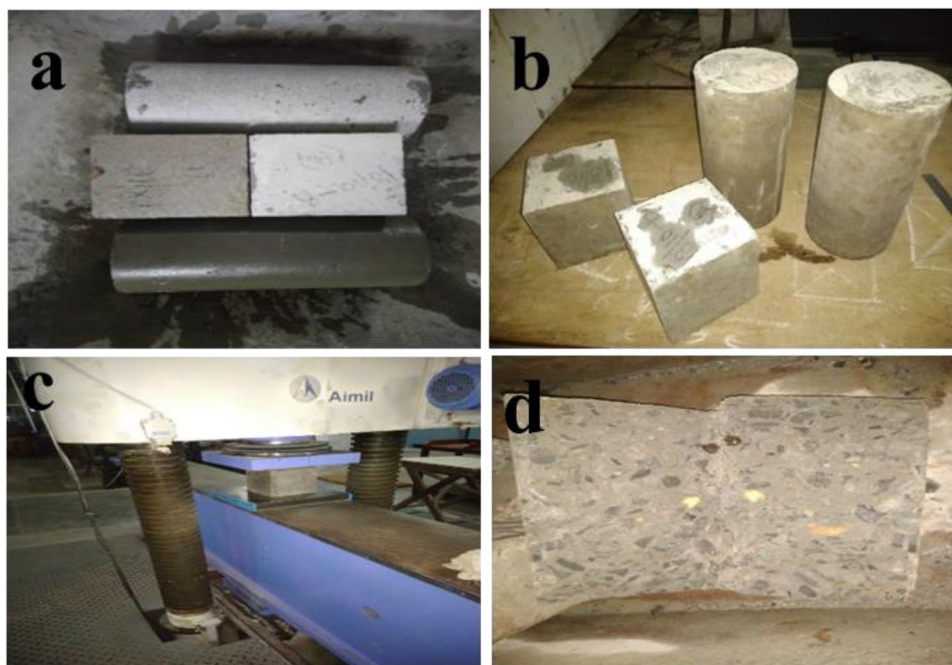
their study, where the introduction of bacterial endospores resulted in the precipitation of calcium carbonate inside the concrete decreased the permeable microvoids of concrete. The resultant reduction of microvoid permeability of concrete resulted in enhanced compressive strength. Another study by Ahmed et al. (2021) showed the improved durable properties of bioconcrete designed with *Bacillus subtilis* and *Bacillus megaterium* cells. Their study also found out that the bacterial cells inside the concrete produce nanosized calcium carbonate biominerals that enhances the mechanical properties of concrete. Later in this study also, it has been found out that the calcite biominerals are formed in the form of nanoparticles that is causing the strength of bioconcrete to enhance.

The tensile strength of bioconcrete with respect to control normal concrete increased to $22 \pm 0.1\%$ on the 3rd day lasting at $14 \pm 0.5\%$ surge at the end of 28 days. Both the cases at the end of 28 days of curing period, the mechanical properties of bioconcrete as compared to normal concrete was significantly higher but the difference of increment reduced.

The possible reason behind this was the compromised viability of the bacterial cells inside the harsh anaerobic environment of the concrete with increasing number of days (Jonkers et al. 2010). Another possible reason was depletion of nutrients, which might be limiting the bacterial cell growth conversely affecting the production of $CaCO_3$ (Mirshahmohammad et al. 2023). Because of these reasons, it is now more sustainable to use bacterial spores which remains dormant for several years (Jose et al. 2018). Another aspect of getting sustained $CaCO_3$ production by microbial cells would be the optimization of nutrient concentration before

adding into concrete mix. Yet another major reason can be non-uniform distribution of biomineral (which were subsequently found in this study to be calcite nanoparticles) as a result of their agglomeration (Mydin et al. 2023) during later stages of biomineralization, which was seen further in this study.

Nevertheless, overall physico-mechanical properties have been improved when using BM RB05 cells for bioconcrete development. Thus, bioconcrete having enhanced performance over conventional concrete was developed as a sustainable alternative.

## Extraction and material characterisation of biomineral produced during MIBM

X-ray diffraction analysis of bioconcrete vs conventional concrete

Both bioconcrete and conventional concrete were characterized chemically to decipher the underlying reason of enhanced performance of bioconcrete. The chemical characterization was done through HR-XRD (Fig. 11a, b) to examine the presence of calcite in the bioconcrete. As observed from Fig. 11a, crystalline peak of calcite at 2θ, 29.5 °C can be seen. A single sharp peak of bioconcrete is due to the presence of calcite at 104 *hkl* plane of calcium carbonate.

This signifies that calcium carbonate formed by the bacterial cells are mostly produced in the form of calcite (Rui and Qian 2022). Also, calcite being the most stable polymorph of calcium carbonate accumulates in its most predominant crystal face at 104 *hkl* plane. Whereas, in the case
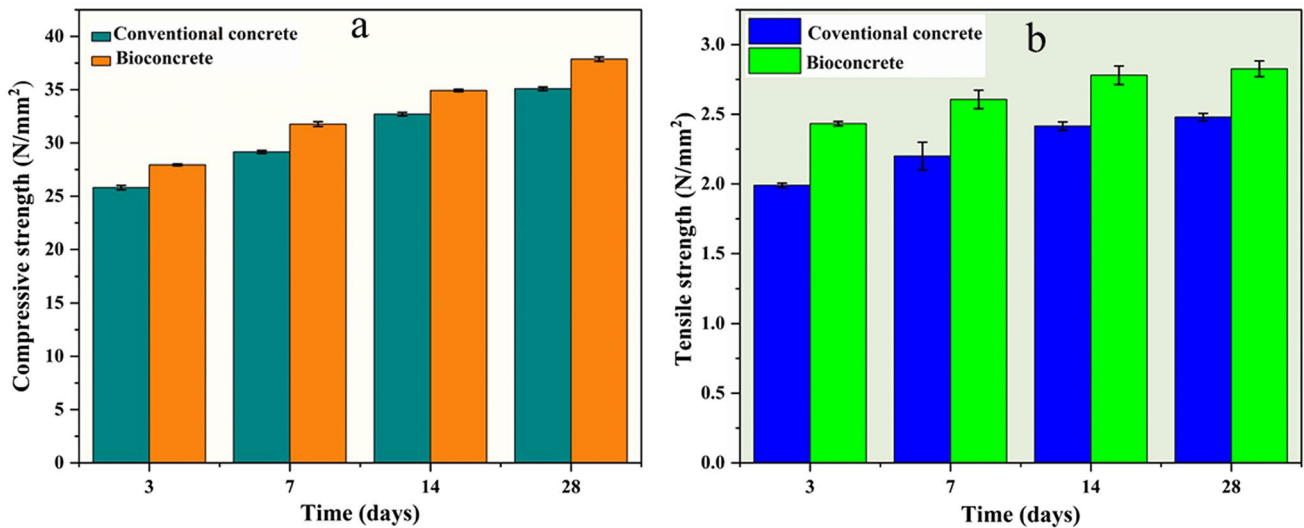
Fig. 10 Bioconcrete vs. conventional concrete. **a** Compressive strength. **b** Spilt tensile strength
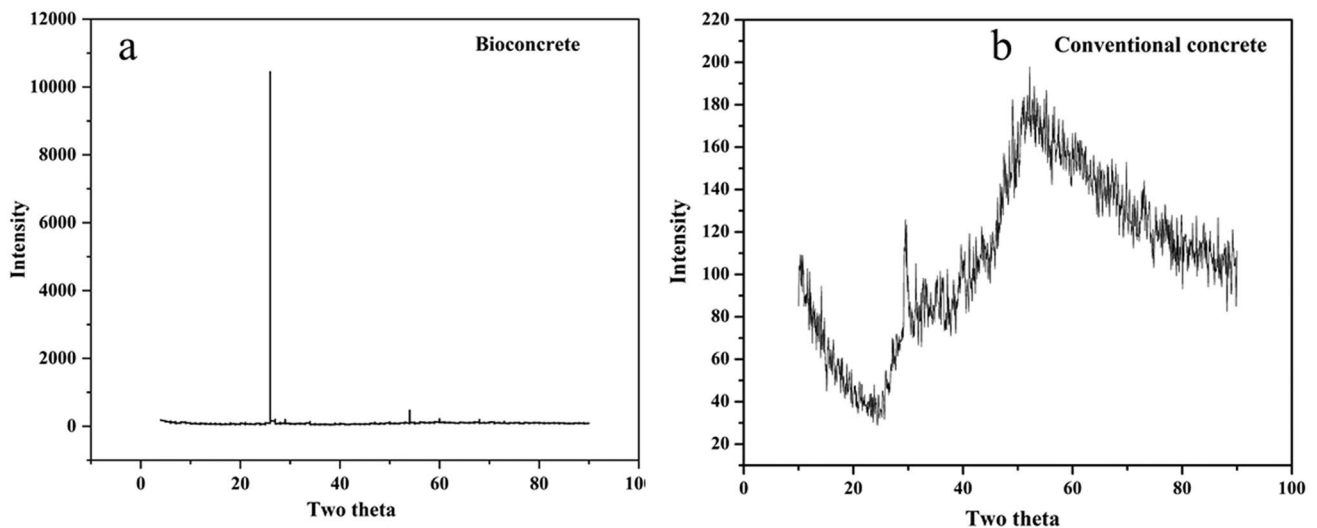
Fig. 11 X-ray diffractograms of **a** Bioconcrete **b** Conventional concrete

of conventional concrete, no such crystalline peak of calcite was seen; instead, amorphous nature of the concrete was observed. Thus, it was said that the increased strength of the bioconcrete is due to the production of calcite nanoparticles by the cells of *Bacillus megaterium* RB05 in the form of calcite inside the concrete. Because there were no bacterial cells in traditional concrete, calcite nanoparticles did not form, leading to a lack of improved mechanical properties. Thus, the reason behind the enhanced strength of bioconcrete over conventional concrete can be deciphered as the formation of calcite by the bacterial cells inside bioconcrete.

Elemental composition by energy dispersive X-ray analysis

The biomineral precipitates were analyzed through EDAX to determine its elemental composition in order to chemically characterize it. The EDAX spectrum (Fig. 12) of the biomineral shows the presence of three major elements.

C, O, and Ca are the major elements which appeared on EDAX analysis of the biomineral. This shows that biomineral is majorly composed of calcium carbonate, which the bacterial cells produce extracellularly through a series of metabolic reactions (Anbu et al. 2016). Further, calcium carbonate appears in multiple polymorphic phases each phase having different properties and stability (Radha et al. 2010).

Fig. 12 EDAX spectrum of precipitated biomineral showing its elemental composition

Lsec: 9.8 0 Cnts 0.000 keV Det: Octane Plus Det
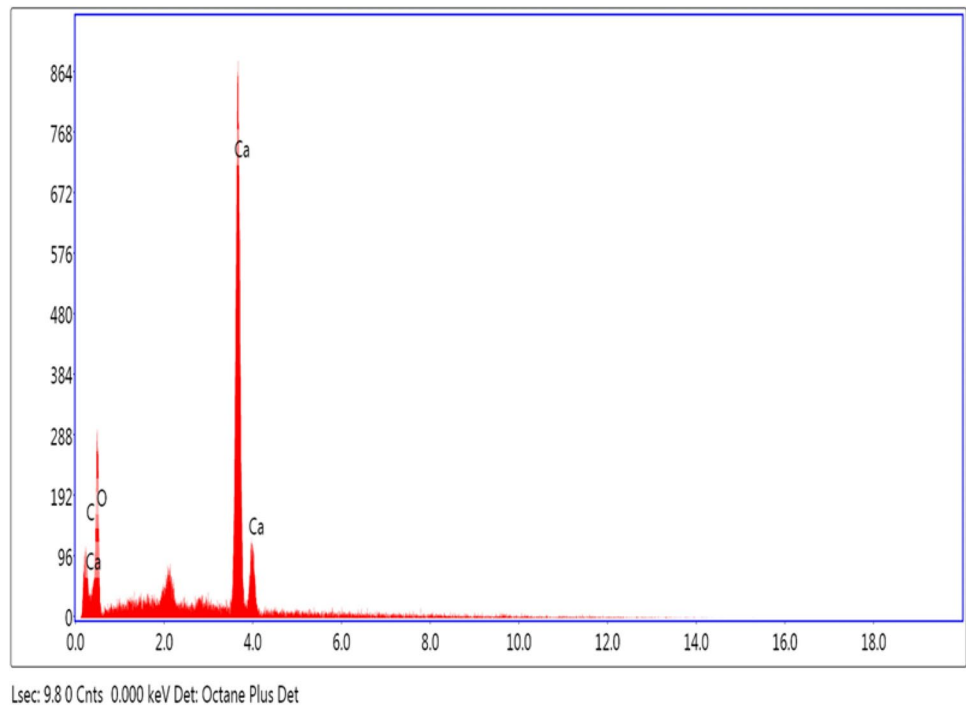
This study in later sections elaborates in detail the polymorphic phase of the biomineral obtained after microbial biomineralization.

Transmission electron microscopy

To analyze the particle size of the biomineral, transmission electron microscopy was performed. It was seen that the biomineral particles had size range variation from 27 to 82 nm (Fig. 13a), signifying that these biominerals falls under the category of nanoparticles. This size range was observed during the onset of biomineralization, on further progression of time these nanoparticles aggregated to form larger particles of size above 100 nm.

As observed from Fig. 13a, the biomineral particles, which can be termed as calcite nanoparticles (calcite nps) starts to appear as single crystals. This was followed by 7th day (Fig. 13b) where these calcite nps was seen embedded on to a matrix-like structure which corresponds to the low electron absorbing organic moieties of bacterial cell wall EPS (Jroundi et al. 2017; Debnath et al. 2023) on reaching 14 days aggregates of biomineral forms comprising of calcite nps (Fig. 13c). Figure 13d shows particle size distribution of calcite nps in the biomineral precipitate; majority of the particles lie below 100 nm as seen from the results. Also, it was seen numerous particles exceeded the nanoscale range, mostly due to aggregation amongst each other. Moreover, it can be said that the high surface to volume ratio of calcite nps (Fig. 13a–c) enhances the mechanical properties of the

concrete by uniform volume distribution in the microvoids present throughout the concrete structure. The resulting decreased pore size reduces water absorptivity by the concrete (Mydin et al. 2023), thereby improving the mechanical properties of it. Also, from the TEM (Fig. 13a–c) results, it can be said that during the initial period of biomineralization, the calcite biomineral was formed in the size of nanoparticles as single crystals, thus this ensured the uniform volume distribution across the microvoids that resulted in higher strength gain of bioconcrete during initial curing period. Whereas, in later stages of biomineralization, the calcite nanoparticles were seen to be agglomerating with each other (Fig. 13c) that caused nonuniform volume distribution across the concrete in the later days of curing. This explains the variation of difference of strength of bioconcrete in 28 days of curing period. The results of strength enhancement of bioconcrete can be well corroborated with the particle size dynamics of the biominerals formed in the microvoids of concrete.

Fourier transform infrared spectroscopy for determination of functional groups

The functional groups of the biomineral were determined to analyze the abundance of different polymorphic phases of the biomineral (Fig. 14). Bands at wavenumber 3430, 2683, 2500 cm^{-1} corresponds to O–H stretch of carboxyl groups present in biomacromolecules like polysaccharides and proteins (Khanjani et al. 2021; Debnath et al. 2023). The presence of these functional groups in the biomineral suggests
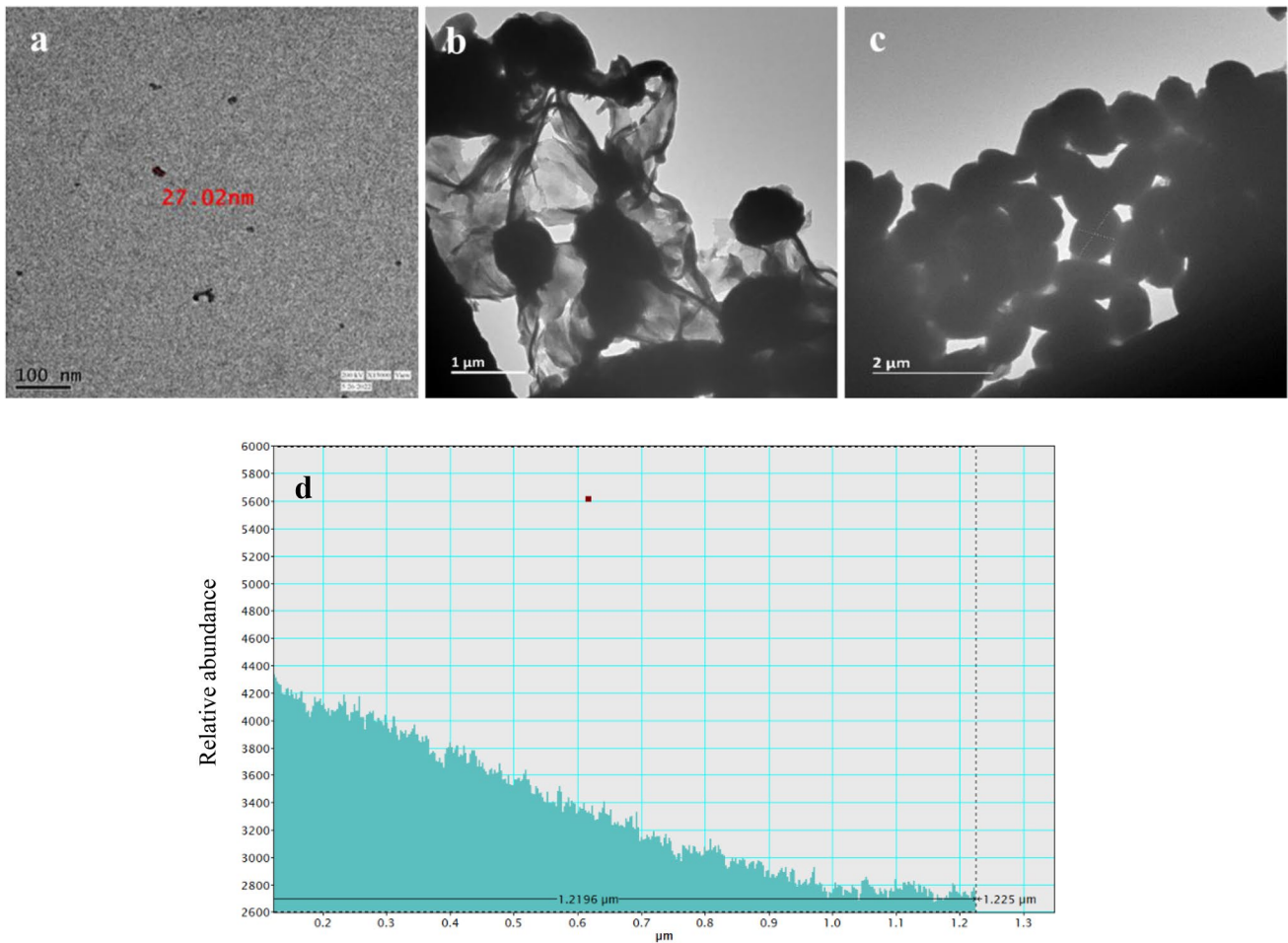
Fig. 13 TEM micrographs of biomineral at different curing period (days). **a** 3, **b** 7, **c** 14, and **d** particle size distribution of biomineral in concrete

the possible association of these biomacromolecules with the biomineral. This could also be corroborated with the TEM data (Fig. 13b), where a matrix-like structure was seen to be attached with calcite nps.

The biomacromolecules corresponds to the EPS produced by the bacterial cells, which acts as template for biomineralization (Enyedi et al. 2020; Khanjani et al. 2021; Debnath et al. 2023). Band at wavenumber at 1469 cm^{-1} corresponds to absorption due to carbonate group, at 1080 cm^{-1} due to symmetric carbonate stretching of amorphous $CaCO_3$ (Khanjani et al. 2021). Band at wavenumber 858 cm^{-1} can be due to the out of plane bending of carbonate (Khanjani et al. 2021; Debnath et al. 2023), which detects the presence of either calcite or vaterite. Band at wavenumber 711 cm^{-1} confirms the in plane bending of calcite (Khanjani et al. 2021). The functional groups associated with the insoluble precipitates produced by the bacterial cells can confirm the production of calcite nps by this process. The organic–inorganic hybrid nature of the biomineral or biocement attributes to the higher strength of the bioconcrete.
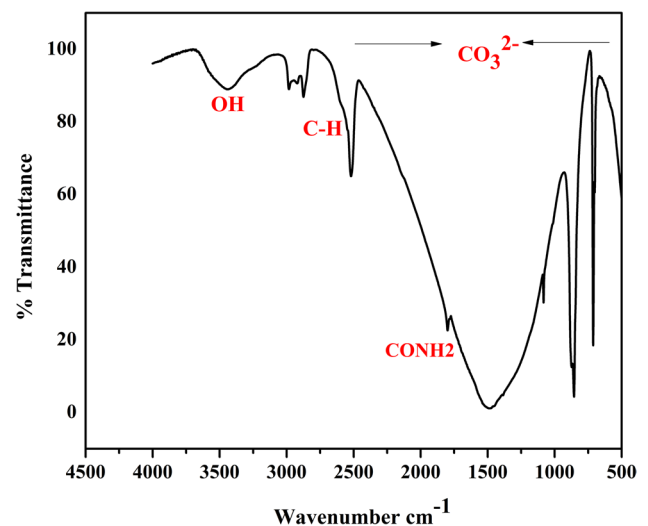
Fig. 14 FTIR spectrum of calcite nps produced extracellularly by bacterial cells

This is in accordance with the hard and durable nature of sea shells, where presence of biomacromolecules provides strength to the inorganic calcium carbonate (Wegst et al. 2015). It has been known that proteinaceous molecules present in the naturally occurring molecules have evolved over time to make these structures durable and hard to break; it is interesting to decipher that microbial biominerals are also of similar nature with microbial extracellular polysaccharides and proteins conferring strength to the biomineral. Thus, the bioconcrete structures developed as a result of microbial biomineral precipitation are of improved mechanical properties with much higher strength as compared to conventional concrete structures.

Bioconcrete vs. conventional concrete

As observed from the results of this study, bioconcrete has proved to be more efficient over conventional concrete in terms of mechanical properties. Both the compressive and spilt tensile strengths were enhanced throughout the curing period. Although the increment of strength reduced slightly with curing time, the mechanical properties of bioconcrete remained higher than conventional concrete till the end of curing. In addition to having enhanced strength, the bioconcrete has an advantage of self-healing, which is lacking in case of conventional concrete. This self-healing property of bioconcrete makes it both environmentally and economically sustainable as the maintenance cost of concrete gets reduced as it can heal its own microcracks. The manufacturing cost would be still higher for bioconcrete but that could be easily replenished by the minimal maintenance cost (Peplow 2020). All in all, bioconcrete is the next generation smart material in the construction and building industry that has generated new hopes to tackle the carbon emission problem of this industry. Still, there is a need to explore more indigenous microorganisms that could perform more efficiently inside the harsh environment of concrete to produce biocement.

Conclusion

- The present study has explored the biomineralization potential of two indigenous *Bacilli* strains such as *Bacillus megaterium* RB05 and *Bacillus foraminis* DRG5, which show the former to be a more potent producer of biogenic $CaCO_3$ with 9.06 g/L of precipitation at the end of 120 h.
- *Bacillus megaterium* RB05 cells were able to survive, metabolize, and produce the $CaCO_3$ biominerals under low O_2 conditions of concrete microenvironment.
- Biogenic $CaCO_3$ produced were characterized to be nanoparticles having crystallinity index of 81.28%.

- Moreover, another interesting finding was the occurrence of biogenic calcite nps embedded on a matrix of organic structure mostly corresponding to extracellular polymeric substance (EPS) produced by the bacterial cells during MIBM, suggesting that the strength enhancement of bioconcrete is contributed by the organic moiety of the biomineral.
- The bioconcrete composed of biogenic calcite nps, showed enhanced compressive and spilt tensile strengths of $6.9 \pm 0.2\%$ and $14 \pm 0.5\%$, respectively over conventional concrete at the end of 28 days of curing.
- However, after 3 days of curing $7.69 \pm 0.08\%$ and $22 \pm 0.1\%$ increment of compressive and spilt tensile strength over control was observed.
- The reason behind this decline might be the reduced viability of bacterial cells inside the extreme environment of concrete. Another possible reason could be the agglomeration of the calcite nps causing non-uniform dispersion along the concrete structure, thereby reducing the strength.

Nonetheless, through this study a very efficient and potent bio-cementing bacterial strain was identified, which produced good amount of biomineral in the form of calcite nanoparticles through MIBM, resulting in enhanced mechanical properties of concrete in a very short span of time. Further, this study could be taken up to the next level to assess the potential of *Bacillus megaterium* RB05 cells, in self-healing of concrete, thereby breaking new ground for the production of an alternative cement, for repairing of concrete structures and mitigating one of the major challenges of the construction industry.

Declarations

Ethics approval Not applicable.

Consent to participate Not applicable.

Consent for publication Not applicable.

Competing interests The authors declare no competing interests.

References

Achal V, Pan X (2014) Influence of calcium sources on microbially induced calcium carbonate precipitation by Bacillus sp. CR2. Appl Biochem Biotechnol 173:307–317. https://doi.org/10.1007/s12010-014-0842-1

Ahmed SO, Nasser AA, Abbas RN et al (2021) Production of bio-concrete with improved durability properties using Alkaliphilic Egyptian bacteria. 3 Biotech 11:1–15. https://doi.org/10.1007/s13205-021-02781-0

Alshalif AF, Juki MI, Tajarudin HA, Othman N, Al-Gheethi AA, Shamsudin S, ... Sabah SA (2022) Optimisation of self-healing of bio-foamed concrete bricks pores using Bacillus tequilensis under different temperature and CO2 curing conditions. Sci Rep 12(1):2682. https://doi.org/10.1038/s41598-022-05659-0

Anbu P, Kang CH, Shin YJ, So JS (2016) Formations of calcium carbonate minerals by bacteria and its multiple applications. Springerplus 5:1–26. https://doi.org/10.1186/s40064-016-1869-2

Andreassen JP (2005) Formation mechanism and morphology in precipitation of vaterite - Nano-aggregation or crystal growth? J Cryst Growth 274:256–264. https://doi.org/10.1016/j.jcrysgro.2004.09.090

Benjamin B, Zachariah S, Sudhakumar J, Suchithra TV (2023) Bacterial consortium development and optimization for crack controlling cement mortar. J Build Eng 77:107501. https://doi.org/10.1016/j.jobe.2023.107501

Brink B (2010) Urease test protocol. American Society for Microbiology, pp 1-7

Carter MS, Tuttle MJ, Mancini JA et al (2023) Microbially induced calcium carbonate precipitation by Sporosarcina pasteurii: a case study in optimizing biological CaCO3 precipitation. Appl Environ Microbiol 89. https://doi.org/10.1128/aem.01794-22

Chowdhury SR, Basak RK, Sen R, Adhikari B (2011) Optimization, dynamics, and enhanced production of a free radical scavenging extracellular polysaccharide (EPS) from hydrodynamic sediment attached Bacillus megaterium RB-05. Carbohydr Polym 86:1327–1335. https://doi.org/10.1016/j.carbpol.2011.06.050

Dagliya M, Satyam N, Garg A (2023) Optimization of growth medium for microbially induced calcium carbonate precipitation (MICP) treatment of desert sand. J Arid Land 15(7):797–811. https://doi.org/10.1007/s40333-023-0018-3

Debnath A, Hazra C, Sen R (2023) Insight into biomolecular interaction–based non-classical crystallization of bacterial biocement. Appl Microbiol Biotechnol 107:6683–6701. https://doi.org/10.1007/s00253-023-12736-5

Dhami NK, Reddy MS, Mukherjee A (2013) Bacillus megaterium mediated mineralization of calcium carbonate as biogenic surface treatment of green building materials. World J Microbiol Biotechnol 29:2397–2406. https://doi.org/10.1007/s11274-013-1408-z

Dhami NK, Reddy MS, Mukherjee A (2014) Synergistic role of bacterial urease and carbonic anhydrase in carbonate mineralization. Appl Biochem Biotechnol 172:2552–2561. https://doi.org/10.1007/s12010-013-0694-0

Dubey AA, Dhami NK, Ravi K, Mukherjee A (2023) Erosion mitigation with biocementation: a review on applications, challenges, & future perspectives. Rev Environ Sci Bio/technol 22(4):1059–1091. https://doi.org/10.1007/s11157-023-09674-z

Enyedi NT, Makk J, Kótai L et al (2020) Cave bacteria-induced amorphous calcium carbonate formation. Sci Rep 10:1–12. https://doi.org/10.1038/s41598-020-65667-w

Ghatak S, Manna S, Roy D et al (2013) Sand stabilization with exo-polymeric substance producing bacteria isolated from a naturally cemented site. In: Proc., 67th Canadian Geotechnical Conf. GéoRegina (pp. 1–8)

Gilmour KA, Ghimire PS, Wright J, Haystead J, Dade-Robertson M, Zhang M, James P (2024) Microbially induced calcium carbonate precipitation through CO_2 sequestration via an engineered Bacillus subtilis. Microb Cel Factories 23(1):168. https://doi.org/10.1186/s12934-024-02437-7

Harnpicharnchai P, Mayteeworakoon S, Kitikhun S et al (2022) High level of calcium carbonate precipitation achieved by mixed culture containing ureolytic and nonureolytic bacterial strains. Lett Appl Microbiol 75:888–898. https://doi.org/10.1111/lam.13748

Hoffmann TD, Reeksting BJ, Gebhard S (2021) Bacteria-induced mineral precipitation: A mechanistic review. Microbiol (United Kingdom) 167. https://doi.org/10.1099/mic.0.001049

IEA (2017) World Energy World Energy. https://www.iea.org/news/a-world-in-transformation-world-energy-outlook-2017. Accessed 18 Jan 2024

Jiang L, Jia G, Wang Y, Li Z (2020) Optimization of sporulation and germination conditions of functional bacteria for concrete crack-healing and evaluation of their repair capacity. ACS Appl Mater Interfaces 12(9):10938–10948. https://doi.org/10.1021/acsami.9b21465

Jonkers HM, Thijssen A, Muyzer G et al (2010) Application of bacteria as self-healing agent for the development of sustainable concrete. Ecol Eng 36:230–235. https://doi.org/10.1016/j.ecoleng.2008.12.036

Jose M, Alonso C, Eloir C et al (2018) Improved strength and durability of concrete through metabolic activity of ureolytic bacteria. Environ Sci Pollut Res 25:21451–21458. https://doi.org/10.1007/s11356-017-9347-0

Jroundi F, Schiro M, Ruiz-Agudo E et al (2017) Protection and consolidation of stone heritage by self-inoculation with indigenous carbonatogenic bacterial communities. Nat Commun 8:1–12. https://doi.org/10.1038/s41467-017-00372-3

Karthika S, Radhakrishnan TK, Kalaichelvi P (2016) A review of classical and nonclassical nucleation theories. Cryst Growth Des 16:6663–6681. https://doi.org/10.1021/acs.cgd.6b00794

Khanjani M, Westenberg DJ, Kumar A, Ma H (2021) Tuning polymorphs and morphology of microbially induced calcium carbonate: controlling factors and underlying mechanisms. ACS Omega 6:11988–12003. https://doi.org/10.1021/acsomega.1c00559

Kim G, Kim J, Youn H (2018) Effect of temperature, pH, and reaction duration on microbially induced calcite precipitation. Appl Sci 8. https://doi.org/10.3390/app8081277

Labaran YH, Mathur VS, Muhammad SU, Musa AA (2022) Carbon footprint management: a review of construction industry. Clean Eng Technol 9:100531. https://doi.org/10.1016/j.clet.2022.100531

Li M, Fu QL, Zhang Q, Achal V, Kawasaki S (2015) Bio-grout based on microbially induced sand solidification by means of asparaginase activity. Sci Rep 5(1):1–9. https://doi.org/10.1038/srep16128

Li X, He X, Ren K, Dong H, Lian B (2023) Mechanisms of carbonate precipitation induced by two model bacteria. Chem Geol 628:121461. https://doi.org/10.1016/j.chemgeo.2023.121461

Liang H, Liu Y, Tian B, Li Z, Ou H (2022) A sustainable production of biocement via microbially induced calcium carbonate precipitation. Int Biodet Biodegrad 172:105422. https://doi.org/10.1016/j.ibiod.2022.105422

Meier A, Kastner A, Harries D, Wierzbicka-Wieczorek M, Majzlan J, Büchel G, Kothe E (2017) Calcium carbonates: induced biomineralization with controlled macromorphology. Biogeosci 14(21):4867–4878. https://doi.org/10.5194/bg-14-4867-2017

Mekonnen E, Kebede A, Nigussie A et al (2021) Isolation and characterization of urease-producing soil bacteria. Int J Microbiol 2021. https://doi.org/10.1155/2021/8888641

Mirshahmohammad M, Rahmani H, Maleki M, Abbas K (2023) Performance of biological methods on self - healing and mechanical properties of concrete using S. pasteurii. Environ Sci Pollut Res 30:2128–2144. https://doi.org/10.1007/s11356-022-21811-9

Mortazavi Bak H, Kariminia T, Shahbodagh B et al (2021) Application of bio-cementation to enhance shear strength parameters of soil-steel interface. Constr Build Mater 294:123470. https://doi.org/10.1016/j.conbuildmat.2021.123470

Mydin MAO, Jagadesh P, Bahrami A, Dulaimi A, Özkılıç YO, Abdullah MMAB, Jaya RP (2023) Use of calcium carbonate nanoparticles in production of nano-engineered foamed concrete. J of Mater Res Technol 26:4405–4422

Onyelowe KC, Adam AF, Ulloa N, Garcia C, Andrade Valle AI, Zúñiga Rodríguez MG, Ganasen N (2024) Modeling the influence of bacteria concentration on the mechanical properties of self-healing concrete (SHC) for sustainable bio-concrete structures. Sci Rep 14(1):8414. https://doi.org/10.1038/s41598-024-58666-8

Ortega-Villamagua E, Gudiño-Gomezjurado M, Palma-Cando A (2020) Microbiologically induced carbonate precipitation in heritage materials. Molecules 25:5499

Peplow M (2020) Bioconcrete presages new wave in environmentally friendly construction. Nat Biotechnol 38(7):776–779

Radha AV, Forbes TZ, Killian CE et al (2010) Transformation and crystallization energetics of synthetic and biogenic amorphous calcium carbonate. Proc Natl Acad Sci U S A 107:16438–16443. https://doi.org/10.1073/pnas.1009959107

Reeksting BJ, Hoffmann TD, Tan L, Paine K, Gebhard S (2020) In-depth profiling of calcite precipitation by environmental bacteria reveals fundamental mechanistic differences with relevance to application. Appl Environ Microbiol 86(7):e0273919. https://doi.org/10.1128/AEM.02739-19

Rui Y, Qian C (2022) Characteristics of different bacteria and their induced biominerals. J Ind Eng Chem 115:449–465. https://doi.org/10.1016/j.jiec.2022.08.032

Salomão R, Costa LMM, de Olyveira GM (2017) Precipitated calcium carbonate nano-microparticles: Applications in drug delivery. Adv Tissue Eng Regen Med Open Access 3:336–340. https://doi.org/10.15406/atroa.2017.03.00059

Sarkar M, Maiti M, Xu S, Mandal S (2023) Bio-concrete: unveiling self-healing properties beyond crack-sealing. J Build Eng 74:106888. https://doi.org/10.1016/j.jobe.2023.106888

Sumathi A, Murali G, Gowdhaman D et al (2020) Development of bacterium for crack healing and improving properties of concrete under wet–dry and full-wet curing. Sustain 12:1–20. https://doi.org/10.3390/su122410346

Tourney J, Ngwenya BT (2009) Bacterial extracellular polymeric substances (EPS) mediate CaCO3 morphology and polymorphism. Chem Geol 262:138–146. https://doi.org/10.1016/j.chemgeo.2009.01.006

Wegst UGK, Bai H, Saiz E, Tomsia AP, Ritchie RO (2015) Bioinspired structural materials. Nat Mater 14:23–36. https://doi.org/10.1038/nmat4089

Yu T, Souli H, Péchaud Y, Fleureau JM (2022) Optimizing protocols for microbial induced calcite precipitation (MICP) for soil improvement–a review. Eur J Environ Civ Eng 26:2218–2233. https://doi.org/10.1080/19648189.2020.1755370

Zheng T, Su Y, Zhang X et al (2020) Effect and mechanism of encapsulation-based spores on self-healing concrete at different curing ages. ACS Appl Mater Interfaces 12:52415–52432. https://doi.org/10.1021/acsami.0c16343

Zhu T, Dittrich M (2016) Carbonate precipitation through microbial activities in natural environment, and their potential in biotechnology: a review. Front Bioeng Biotechnol 4:1–21. https://doi.org/10.3389/fbioe.2016.00004

Zoheir AE, Hammad IA, Talkhan FN (2013) Urease activity and induction of calcium carbonate precipitation by Sporosarcina pasteurii NCIMB 8841. J Appl Sci Res 9:1525–1533